The influence of local field corrections on Thomson scattering in non-ideal two-component plasmas

Carsten Fortmann, August Wierling, and Gerd Röpke*
Universität Rostock, Institut für Physik, 18051 Rostock, Germany
(Dated: June 19, 2009)

Thomson scattering in non-ideal (collision-dominated) two-component plasmas is calculated accounting for electron-ion collisions as well as electron-electron correlations. This is achieved by using a novel interpolation scheme for the electron-electron response function generalizing the traditional Mermin approach. Also, ions are treated as randomly distributed inert scattering centers. The collision frequency is taken as a dynamic and complex quantity and is calculated from a microscopic quantum-statistical approach. Implications due to different approximations for the electron-electron correlation, i.e. different forms of the OCP local field correction, are discussed.

I. INTRODUCTION

Recently, Thomson scattering has been established as a diagnostic tool for high energy laser-matter interaction in particular for warm dense matter [1, 2, 3, 4]. The Thomson signal probes the dynamic structure factor of the plasma [5]. Reversing the argument, we can synthesize the Thomson signal by using an appropriate expression for the dynamic structure factor and infer density and temperature conditions by matching the synthesized signal to the experimental one. In particular, at high densities, collisions and correlations have to be accounted for in modeling $S(k,\omega)$ [6]. The Mermin approximation [7] has been found to be a simple way of interpolating between the collision-less plasma (RPA) at large wavevectors and collisions in the long wavelength limit, i.e. a Drude-like expression for the dielectric function. However, in non-ideal plasmas, correlations beyond the RPA exist even at finite values of k and have to be taken into account. The traditional Mermin approach fails to incorporate these correlations. An interpolation scheme between static local field corrections and the Drude model by a generalized Mermin approach has been suggested in Ref. [8] using the Zubarev approach to the non-equilibrium statistical operator [9, 10]. This scheme guarantees the correct account of electron correlations in the static limit.

Having an interpolation scheme at our disposal, a systematic study of the influence of both electron-ion collisions as well as electron-electron correlations is possible. It is the objective of this paper to contribute to such a study. In particular, since the correct form of the dynamic as well as the static local field corrections for the interacting electron gas is still a matter of debate, we compare a few recent suggestions in their consequences for the Thomson scattering signal.

The paper is organized as follows. In Sec. II, we give a brief review of the formalism and the approach to the dynamic collision frequency. Sec. III in some detail explains the different models for the dynamic local field correction considered here. Results for the plasmon dispersion are discussed in Sec. IV. Finally, conclusions and an outlook complete this paper.

II. THEORETICAL BACKGROUND

We consider a neutral plasma of electrons and ions in thermal equilibrium with electron density n_e, ion density $n_i = n_e$ and temperature T. For later use, we introduce the Fermi wave vector $k_F = (3\pi^2 n_e)^{1/3}$, the Fermi energy $E_f = \hbar^2 k_F^2/(2m_e)$, and the Brueckner parameter r_s given by $(4\pi/3)n_e a_{\rm B}^3 r_s^3 = 1$, where $a_{\rm B}$ is Bohr's radius. These parameters are relevant in our context, because we use the model of an electron gas at $T = 0$ interacting with an inert background of ions in carrying out our exploratory calculations.

*Electronic address: august.wierling@uni-rostock.de

A. Thomson scattering and Born-Mermin approach

It is well-known, see [2, 3, 4], that the experimental Thomson scattering cross section is related to the dynamic structure factor of all electrons in the plasma according to

$$\frac{d^2\sigma}{d\Omega d\omega} = \sigma_T \frac{k_1}{k_0} S_{ee}(k,\omega) \ . \tag{1}$$

In this expression, $\sigma_T = 6.65 \times 10^{-29}\,\mathrm{m}^2$ is the Thomson cross section, and k_0 and k_1 are the wavenumbers of the incident and the scattered light. The energy and momentum transfer are given by $\Delta E = \hbar\omega = \hbar\omega_1 - \hbar\omega_0$ and $\hbar\mathbf{k} = \hbar\mathbf{k}_1 - \hbar\mathbf{k}_0$. The momentum is related to the scattering angle θ_s in the limit $\hbar\omega \ll \hbar\omega_0$ by $k = 4\pi\sin(\theta_s/2)/\lambda_0$ for an incident wavelength λ_0. Here, we follow Chihara' s approach [5], in that the total dynamic structure factor can be written in terms of contributions from free electrons , weakly and tightly bound electrons, and core electrons. In this paper, only the dynamic structure factor of free electrons is considered.

In thermodynamic equilibrium, the dynamic structure factor $S_{ee}(k,\omega)$ and the longitudinal response function $\chi_{ee}(k,\omega)$ are related via the fluctuation-dissipation theorem

$$S_{ee}(k,\omega) \ = \ -\frac{1}{\pi n_e} \frac{1}{1-\mathrm{e}^{-\hbar\omega/(k_B T)}} \,\mathrm{Im}\,\chi_{ee}(k,\omega) \ . \tag{2}$$

Theoretical approaches to dynamic structure factor of two-component plasmas have been developed starting from different approaches such as perturbation theory, the viscoelastic model [11], the recurrence relation method [12], or the moment approach, see Ref. [13]. As an example for a perturbative treatment, we mention Ref. [14, 15]. There, based on the generalized linear response theory of Zubarev, a systematic account of correlations as well as collisions has been accomplished by partial summation of diagram classes using thermodynamic Green's functions. While a detailed evaluation of the resulting expressions for the response functions is cumbersome at arbitrary wave vectors k, numerical calculations have been carried out in the long-wavelength limit $k \to 0$. In particular, approximative expressions for the collision frequency $\nu(\omega)$ have been studied taking care of strong collisions as well as dynamical screening in a consistent manner.

To generate approximative results for the response function at finite wave vectors k, we follow an idea suggested by Mermin [7]. Ensuring particle number conservation by introducing local thermal equilibrium together with a relaxation time ansatz, the electron-electron response function is approximated by

$$\chi^{(M)}(k,\omega) \ = \ \left(1-\frac{i\omega}{\eta}\right) \frac{\chi_{\mathrm{ee}}^{\mathrm{RPA}}(k,\omega+i\eta)\,\chi_{\mathrm{ee}}^{\mathrm{RPA}}(k,0)}{\chi_{\mathrm{ee}}^{\mathrm{RPA}}(k,\omega+i\eta) - \frac{i\omega}{\eta}\chi_{\mathrm{ee}}^{\mathrm{RPA}}(k,0)} \ , \tag{3}$$

with a relaxation parameter η. For details, see Ref. [10]. Here, $\chi_{\mathrm{ee}}^{\mathrm{RPA}}$ is the electron response function in random phase approximation, i.e.

$$\chi_{\mathrm{ee}}^{\mathrm{RPA}}(k,\omega) \ = \ \frac{\chi^{(0)}(k,\omega)}{1 \ - \ V(k)\chi^{(0)}(k,\omega)} \tag{4}$$

where $\chi^{(0)}(k,\omega)$ is the ideal, i.e non-interacting response function , see [16]. For $T = 0$, this ideal response can be found as

$$V(k)\chi^{(0)}(k,\omega) \ = \ -\frac{\chi_0^2}{4z^3}\,\left[g(u+z) - g(u-z)\right] \ , \tag{5}$$

with $u \ = \ m\omega/(\hbar k\, k_F)$, $z \ = \ k/(2\,k_F)$, $\chi_0^2 \ = \ (\pi k_F a_{\mathrm{B}})^{-1}$ and

$$g(x) \ = \ x + \frac{1}{2}\left(1-x^2\right)\,\ln\frac{x+1}{x-1} \ , \tag{6}$$

$$\tag{7}$$

The function $g(x)$ given here is a generalization of the function $g(x)$ given in [16] to complex arguments. Furthermore $V(k)$ denotes the Coulomb-potential in momentum space. Note, that Eq. (3) reduces to the RPA expression in the absence of collisions, i.e. $\eta = 0$. Also, in the long-wavelength limit, Eq. (3) turns into the familiar Debye form, allowing to identify the relaxation parameter η as the collision frequency $\nu(\omega)$.

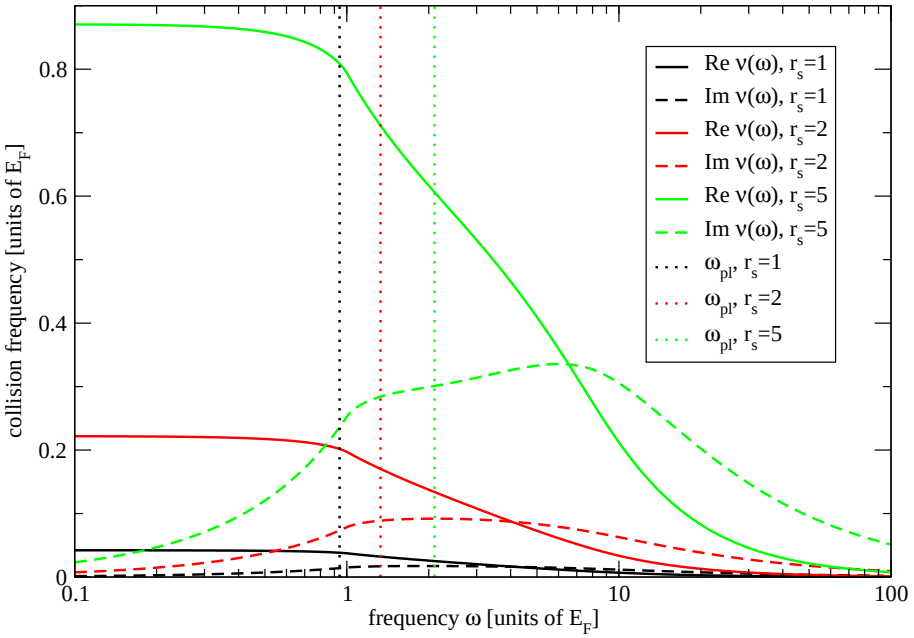

FIG. 1: Real part of the collision frequency $\nu(\omega)$ as a function of the frequency ω. Various values of the Brueckner parameter r_s are considered.

B. Extended Mermin approach

To account for correlations among the electrons, an extension of the traditional Mermin expression has been suggested, see Ref. [8]. For an adiabatic model with inert ions, it reduces to replacing the RPA response function in Eq. (3) by the response function of the interacting one-component (OCP) electron gas $\chi_{ee}^{\rm OCP}(k,\omega)$,

$$\chi_{ee}^{\rm (xM)}(k,\omega) \;=\; \left(1-\frac{i\omega}{\eta}\right)\left(\frac{\chi_{ee}^{\rm OCP}(k,\omega+i\eta)\,\chi_{ee}^{\rm OCP}(k,0)}{\chi_{ee}^{\rm OCP}(k,\omega+i\eta)\;-\;(i\omega/\eta)\,\chi_{ee}^{\rm OCP}(k,0)}\right)\;, \tag{8}$$

where the label xM indicates the extended Mermin expression for the response function. Note, that the same expression has been derived independently by Barriga-Carrasco [17]. Traditionally, the OCP response function is represented using a dynamic local field correction $G_{ee}(k,\omega)$ as

$$\chi_{ee}^{\rm OCP}(k,\omega) \;=\; \frac{\chi_e^{(0)}(k,\omega)}{1-V(k)\,(1-G_{ee}(k,\omega))\,\chi_e^{(0)}(k,\omega)}\;. \tag{9}$$

Having a collision-less plasma $\nu=0$, the response function is solely the OCP expression. Due to the fact, that electron-electron collisions do not contribute in the long-wavelength limit, i.e. $G_{\rm ee}(k,\omega)\propto k^2$ for $k\to 0$, this expression still reduces to the Drude-like form for small k with the same $\nu(\omega)$ as before. However, contrary to Eq. (3), the static limit is now given by the electron-electron correlation in the OCP,

$$\lim_{\omega\to 0}\chi_{ee}^{\rm (xM)}(k,\omega) \;=\; \chi_{ee}^{\rm OCP}(k,0)\;. \tag{10}$$

C. Collision frequency at arbitrary degeneracy

For the exploratory calculation discussed here, we use the collision frequency in Born approximation and for arbitrary degeneracy, see Ref. [15],

$$\mathrm{Re}\,\nu(\omega) \;=\; \frac{\epsilon_0 n_i \Omega_0^2}{6\pi^2 e^2 n_e m_e}\int_0^\infty dq\,q^6\,V_{\rm TF}(q)^2\,S_i(q)\,\frac{1}{\omega}\mathrm{Im}\,\epsilon_{\rm RPA,e}(q,\omega)\;, \tag{11}$$

where $V_{\rm TF}(q)=V(q)/\epsilon^{(RPA)}(q,0)$ is the static screened potential, $S_i(q)$ is the static structure factor of the ions, taken e.g. in HNC approximation or from MD simulations, Ω_0 is a normalization volume, and $\epsilon_{\rm RPA,e}(q,\omega)$ is the dielectric

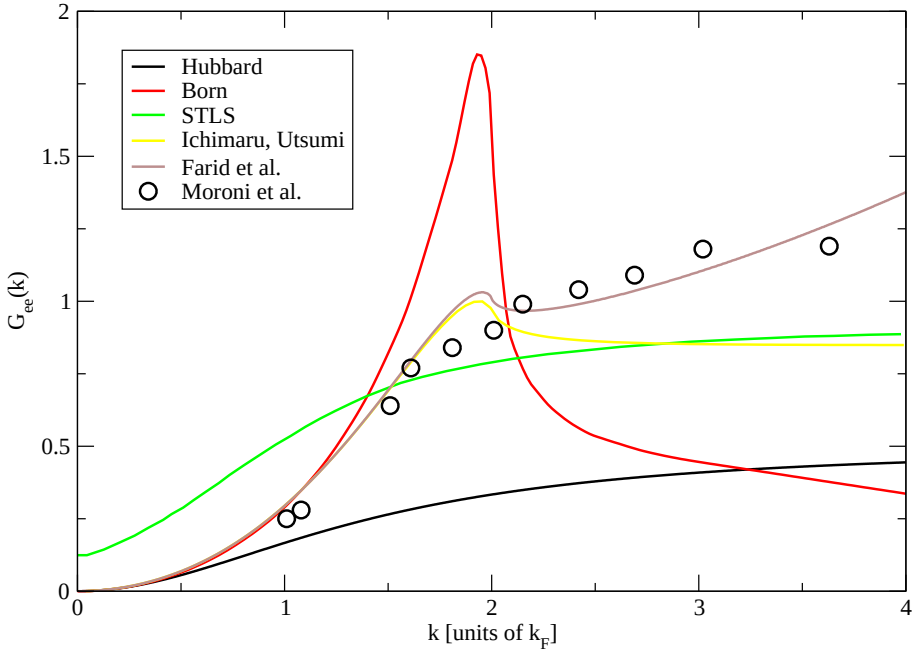

FIG. 2: Static local field correction $G_{\rm ee}(k)$ for $r_s = 2$. Approximations: Hubbard [18], Born [22], STLS [23], Utsumi and Ichimaru [19], Farid et al. [20], Moroni et al. [24].

function of the electron OCP for arbitrary degeneracy as given e.g. in the article of Arista and Brandt [16]. Again, we determine the RPA dielectric function for $T = 0$ by using Eq. (5).

We restrict ourselves to this easily accessible expression since we want to focus on the interplay between collisions and electron-electron correlations and the rôle of different approximations for the OCP local field corrections. More advanced expressions are given in Ref. [15] and should be used for realistic calculations. Also, realistic calculations should include electron-electron effects on the collision frequency, which can be taken into account by increasing the number of moments in linear response approach, see Ref. [15] as well.

In Fig. 1, we show the collision frequency $\nu(\omega)$ as a function of the frequency ω for three different values of the Brueckner parameter $r_s = 1, 2, 5$. Note, that $\nu(\omega)$ is a complex quantity and the imaginary part is connected to $\mathrm{Re}\,\nu(\omega)$ by a Kramers-Kronig relation

$$\mathrm{Im}\,\nu(\omega) \;=\; \int_{-\infty}^{\infty} \frac{d\omega'}{\pi}\, \frac{\mathrm{Re}\,\nu(\omega')}{\omega - \omega'} \quad . \tag{12}$$

The account of this imaginary part is essential for obeying both, the f-sum sum rule and the perfect screening sum rule. While loosely speaking, the real part leads to a broadening of the plasmon at $k = 0$, the imaginary part produces a shift of the plasmon. For a static frequency $\omega = 0$, the imaginary part vanishes, i.e. replacing the dynamic by a static collision frequency $\nu(0)$ one ignores the shift of the plasmon position.

III. LOCAL FIELD CORRECTIONS FOR AN INTERACTING ELECTRON GAS AT $T = 0$

A. Static local field correction for the OCP

In an often used approximation, the dynamics in the local field correction is ignored reducing it to the static limit only,

$$\chi_{\rm ee}^{\rm OCP}(k,\omega) \;=\; \frac{\chi_e^{(0)}(k,\omega)}{1 - V(k)\,(1 - G_{\rm ee}(k))\,\chi_e^{(0)}(k,\omega)} \quad . \tag{13}$$

For the static local field correction $G_{\rm ee}(k)$, a plethora of approximations have been suggested beginning with the original paper by Hubbard [18]. Here, it is impossible to give an exhaustive review. Instead, we concentrate to the

widely-used expression of Ichimaru and Utsumi [19] and its extension by Farid et al. [20]. For an overview of other approximations, see Ref. [21]. For the sake of illustration, we compare a few approximations in Fig. 2 for $r_s = 2$, see [22, 23]. Also included are results obtained with a Monte Carlo (MC) simulation by Moroni et al. [24]. Qualitatively similar results are obtained for other values of r_s. For small values of k, the Utsumi-Ichimaru approximation and the extended model of Farid et al. are identical by construction and adapted to the compressibility sum rule. There is a good agreement with the MC data and both, the Utsumi-Ichimaru and the Farid et al. description, while the other approximations do not describe these so well. In the deep inelastic regime at large k, Farid et al. take account of the results by Holas [25], that $G_{\rm ee}(k)$ scales as k^2, which is not included into the Utsumi-Ichimaru ansatz. The MC data seem to support this k^2 scaling. For our discussion, this difference is rather unimportant, since the plasmon ceases to be a well-defined mode at $k_0 \leq k_F$, while the differences between Ichimaru-Utsumi and Farid et al. arise for $k \gtrsim 2k_F$.

B. Dynamic local field corrections for the OCP

As already mentioned, there are several approximative approaches to the dynamic structure factor of the electron gas. Here, we use the approach of Dabrowski [26] and the approach of Hong and Lee [27]. Both approaches are interpolation schemes incorporating sum rules and other exact properties. In particular, the static properties are inputs into these schemes and we can use the local field correction of Farid et al. again in this case. This would have been impossible if we choose the perturbative results of e.g. Richardson and Ashcroft [28].

Being a dynamical quantity, the local field correction is also a complex quantity obeying Kramers-Kronig like relations. For the real part $\mathrm{Re}\, G_{\rm ee}(k,\omega)$ of the dynamic local field correction, the static limit is just approximated by $G_{\rm ee}(k)$ given above. The high frequency asymptotics is given by three-frequency sum rule and therefore by the static structure factor and the correlated kinetic energy of the electron gas, see Ref. [29, 30],

$$\lim_{\omega\to\infty} G_{\rm ee}(k,\omega) \;=\; I(k) \;-\; \frac{2k^2}{m\omega_{\rm pl}^2}\left(\langle E_{\rm kin}\rangle \;-\; \langle E_{\rm kin}\rangle_0\right) \tag{14}$$

which in turn is given by the static structure factor $S(k)$

$$I(k) \;=\; -\frac{1}{N}\sum_{\vec{q}\neq\vec{k},\vec{0}} K\left(\vec{k},\vec{q}\right)\left(\vec{k}\cdot\vec{q}\right)^2\left[S(|\vec{q}-\vec{k}|) \;-\; 1\right] \quad , \tag{15}$$

and

$$K(\vec{k},\vec{q}) \;=\; \frac{\vec{q}\cdot\vec{k}}{k^2} \;+\; \frac{\vec{q}\cdot\left(\vec{q}-\vec{k}\right)}{|\vec{q}-\vec{k}|^2} \quad . \tag{16}$$

Furthermore, $\langle E_{\rm kin}\rangle$ is the kinetic energy of the interacting electron gas, $\langle E_{\rm kin}\rangle_0$ its non-interacting counterpart, $\omega_{\rm pl}$ is the plasma frequency.

Also, Dabrowski incorporates the perturbative result of Glick and Long [31] for the high-frequency behavior of the imaginary part of the dynamic structure factor. He extends a Padé approximation suggested by Gross and Kohn [32] to finite values of the wave vector,

$$\mathrm{Im}\, G_{\rm ee}(k,\omega) = \frac{a(k)\omega}{(1+b(k)\omega^2)^{5/4}} \tag{17}$$

with

$$a(k) \;=\; Ck^2\left(\frac{\mathrm{Re}\, G_{\rm ee}(k,0) \;-\; \mathrm{Re}G_{\rm ee}(k,\infty)}{CDk^2}\right)^{5/3} \quad , \tag{18}$$

$$b(k) \;=\; \left(\frac{\mathrm{Re}\, G_{\rm ee}(k,0) \;-\; \mathrm{Re}\, G_{\rm ee}(k,\infty)}{CDk^2}\right)^{4/3} \quad , \tag{19}$$

and $C = 23/66\,\alpha\, r_s$, $D = \Gamma(3/4)/(\sqrt{\pi}\,\Gamma(5/4)) \approx 0.763$, $\alpha = (4/(9\pi))^{1/3}$. The corresponding real part is then obtained by a Kramers-Kronig relation,

$$\mathrm{Re}\, G_{\rm ee}(k,\omega) \;=\; \mathrm{Re}\, G_{\rm ee}(k,\infty) \;+\; P\int_{-\infty}^{\infty}\frac{d\omega'}{\pi}\,\frac{\mathrm{Im}\, G_{\rm ee}(k,\omega')}{\omega' \;-\; \omega} \quad , \tag{20}$$

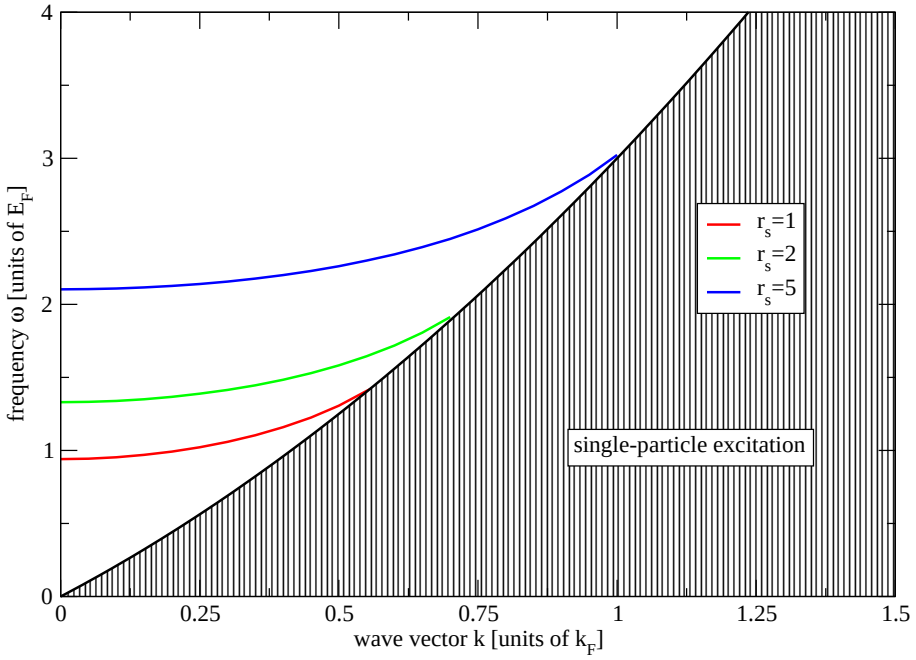

FIG. 3: Plasmon dispersion relation in RPA approximation. Brueckner parameters $r_s = 1, 2, 5$ are considered. The intersection of the plasmon dispersion with the single-particle ridge defines the wave vector $k_0(r_s)$.

where $P\int$ indicates Cauchy principal value integration.

As a second option for the dynamic local field correction of the OCP we introduce the above mentioned approach of Hong and Lee [27, 29], which is based on the recurrence relation technique. Specifically, we use the lowest dynamical extension of the local field correction, which can be introduced by this technique. Adapting the notation to this paper, the dynamical local field correction reads

$$G_{\rm ee}(k,z) \;=\; G_{\rm ee}(k,0) \,+\, \left[G_{\rm ee}(k,\infty) \,-\, G_{\rm ee}(k,0)\right]\, c_2^0(z) \tag{21}$$

with a function c_2^0 given by [33]

$$c_2^0(z) \;=\; \frac{\Delta_1^0}{\Delta_2^0}\left(\frac{\chi^{(0)}(k,0)}{\chi^{(0)}(k,z)} \,-\, 1\right) + \frac{z^2}{\Delta_2^0} \;. \tag{22}$$

Here, the quantities Δ_1^0 and Δ_2^0 are the ideal recurrants $\Delta_1^0 = -\frac{\omega_{\rm pl}{}^2}{V(k)\chi_{\rm ee}^{(0)}(k)}$, $\Delta_2^0 = \left[\frac{12}{5}\left(\frac{k}{k_F}\right)^2 + \left(\frac{k}{k_F}\right)^4\right]\left(\frac{E_F}{\hbar}\right)^2 - \Delta_1^0$.

Both approaches have been adapted in this paper to the most recent results for the static electron-electron structure factor $S(k)$ and the correlated kinetic energy, see Ref. [34]. The details will be covered in an forthcoming publication [35].

IV. COMPARISON OF DIFFERENT APPROXIMATIONS

Instead of showing the dynamical structure factor $S(k,\omega)$ for each of the different approximations and for various values of the wave vector k and the frequency ω, we introduce the plasmon position $\omega(k) = \max_{\omega} S_{\rm ee}(k,\omega)$ and the plasmon width $\Gamma(q)$ as a signature for the influence of different effects, where we measure the width as full width at half maximum (FWHM). In a collision-less plasma at $T = 0$, the plasmon is a well-defined mode for $k < k_0(r_s)$ corresponding to a δ-like spike in the dynamic structure factor. For larger k, the plasmon ceases to be a well-defined mode and shows a broadening even in RPA, see Ref. [16]. We illustrate these dispersion relations in Fig. 3. The wave vector $k_0(r_s)$, where the plasmon dispersion $V(k)\chi^{(0)}(k,\omega) = 1$ intersects with the single-particle ridge $\omega = \hbar k\left(k - 2k_F\right)/2m$ is smaller than k_F for all of the values r_s considered here. Collisions as well as correlations modify these RPA dispersion relations leading to a shift and a broadening of the plasmon even at $k < k_0(r_s)$. For the conditions of warm dense matter, the plasmon dispersion in the traditional Born-Mermin approach has been studied by Thiele et al. [4].

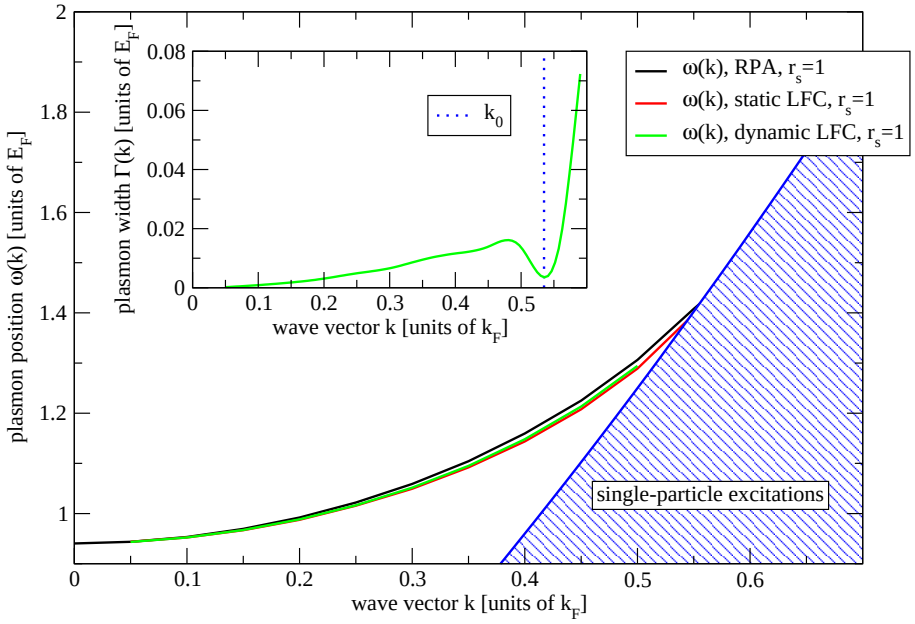

FIG. 4: Plasmon shift $\omega(k)$ and plasmon width $\Gamma(k)$ as a function of the wave vector k. $r_s = 1$ is studied. We compare the static local field correction to the dynamic local field correction. No collisions are included.

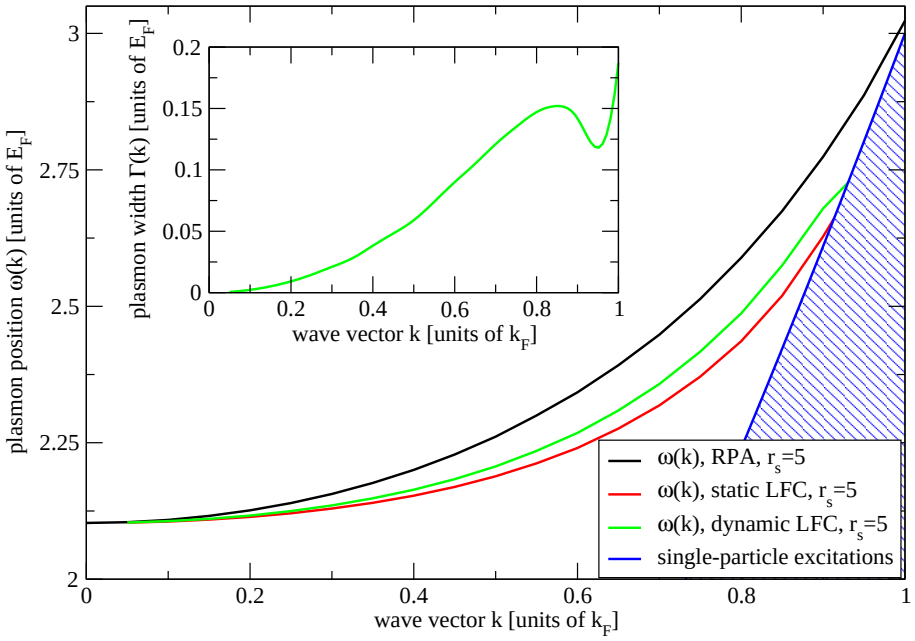

FIG. 5: Plasmon shift $\omega(k)$ and plasmon width $\Gamma(k)$ as a function of the wave vector k. $r_s = 5$ is studied. We compare the static local field correction to the dynamic local field correction. No collisions are included.

A. Plasmon dispersion without collisions

In a first step, we discuss the effects induced only by local field corrections, i.e. for $\nu(\omega) = 0$. The modifications of the plasmon properties are shown in Fig. 4 for $r_s = 1$ and in Fig. 5 for $r_s = 5$. RPA, static local field corrections and dynamic local fields given by the improved Dabrowski interpolation scheme are compared. In the first case, the deviations of the static LFC from the RPA results are quite small. Also, the dynamic LFC is only a minor correction to the static expression. This is consistent with the plasmon width, which is below 1 % for almost all wave vectors k. Note, that the rapid increase above $0.55\,k_F$ is due to the onset of damping in the RPA expression. For $r_s = 5$, the

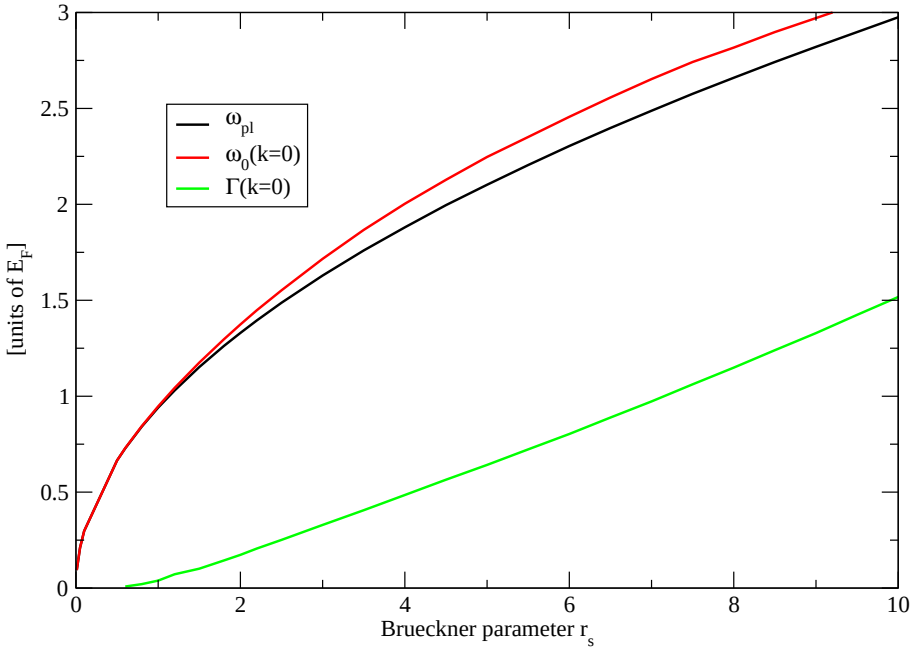

FIG. 6: Plasmon shift $\omega(0)$ and width $\Gamma(0)$ as a function of the Brueckner parameter r_s. Here, we account for electron-ion collisions only using the traditional Born-Mermin approximation of Eq. (3) and Eq. (11). No local field corrections are considered.

noticeable deviations occur. Also, a clear influence of dynamical LFC is visible. This is also reflected in the plasmon damping, where a width of up to 17 % is found.

B. Results for the extended Mermin approach

We start the presentation of the results for the extended Born-Mermin approach by focussing on the long-wavelength limit $k \to 0$. In this limit, the Born-Mermin ansatz reduces to a Drude-type dielectric function with a frequency-dependent and complex collision frequency $\nu(\omega)$. This frequency leads to a broadening and a shift of the plasmon as can be seen from the imaginary part of the inverse dielectric function, which is given by

$$\mathrm{Im}\,\epsilon(k \to 0, \omega) \;=\; -\frac{\mathrm{Re}\,\nu(\omega)\,\omega\,\omega_{\mathrm{pl}}^2}{\left(\omega^2 \,-\, \omega_{\mathrm{pl}}^2 \,-\, \mathrm{Im}\,\nu(\omega)\,\omega\right)^2 \,+\, (\mathrm{Re}\nu(\omega))^2\,\omega^2} \quad . \tag{23}$$

Approximately, for $\mathrm{Re}\,\nu(\omega) >> \mathrm{Im}\,\nu(\omega)$, the real part is connected to a broadening, while the imaginary part induces a shift of the plasmon. Local field corrections do not play any rôle in this limit as discussed above. The shift and the broadening are illustrated in Fig. 6 as a function of the Brueckner parameter r_s. Since the real as well as the imaginary part of $\nu(\omega)$ increase with r_s for the conditions considered here, the broadening $\Gamma(k=0)$ of the plasmon also increases with r_s. For large r_s, the broadening is about half the size of the plasma frequency ω_{pl}. The shift of the plasmon also increases with r_s. However, the shift is less pronounced compared to the width of the plasmon, an effect consistent with $\mathrm{Im}\,\nu(\omega) < \mathrm{Re}\,\nu(\omega)$.

Next, we present the wave vector dependence of the plasmon shift $\omega(k)$ and the plasmon width $\Gamma(k)$. The results for the shift are shown in Fig. 7-9 for $r_s = 1, 2, 5$. Fig. 11 displays the width for $r_s = 5$. We compare three different approximations, the traditional Born-Mermin (BM) given by Eq. (3) and Eq. (11), the extended Born-Mermin approach with static local field correction (BM+sLFC) of Eq. (8) together with Eq. (13) and finally the extended Born-Mermin approach with dynamic local field corrections (BM+dLFC) by the Dabrowski ansatz, i.e. Eq. (17) and Eq. (20). Also, the RPA dispersion relation is shown, with $1 - V(k)\,\chi^{(0)}(k, \omega(k)) = 0$ for $k < k_0$ and the position of the maximum of $\mathrm{Im}\,\chi_{\mathrm{ee}}^{\mathrm{RPA}}(k, \omega)$ for $k > k_0$.

The shift at $k = 0$ shown in these figures corresponds to the values for $r_s = 1, 2, 5$ in Fig. 6. In this limit, the local field corrections do not contribute. Thus, the different approximations merge for $k \to 0$. As in the long-wavelength limit, the deviation of all approximative expressions from the RPA results are more pronounced with increasing r_s.

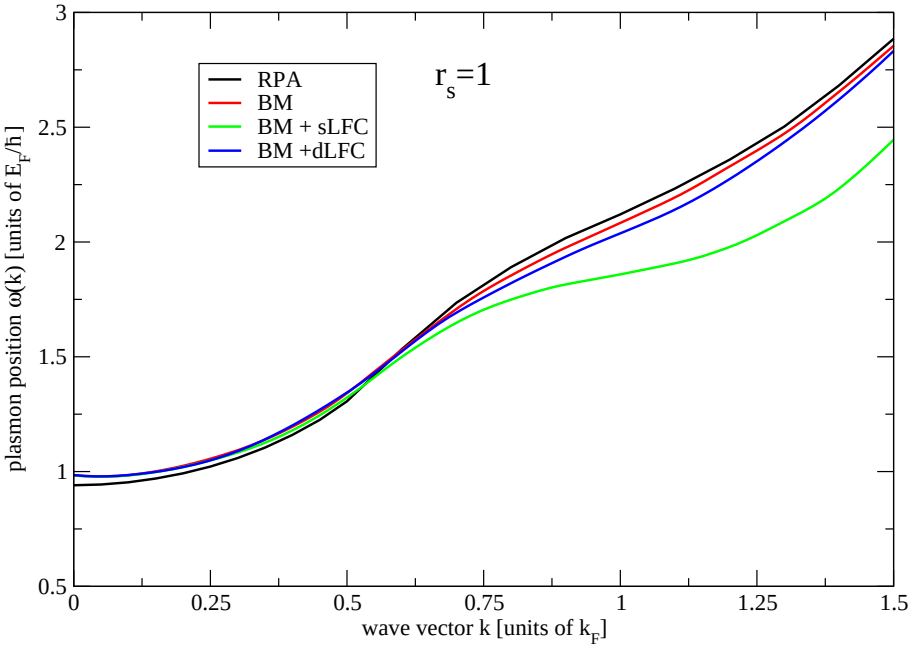

FIG. 7: Plasmon shift $\omega(k)$ as a function of the wave vector k. $r_s = 1$ is studied. BM: traditional Born-Mermin approximation. BM + sLFC: Born-Mermin including static local field corrections. BM + dLFC: Born-Mermin including dynamic local field corrections.

As for the Born-Mermin result, it shows a systematic behavior with a switch from a blue shift to a red shift at a value of k close to k_0. Similar results have been reported by Thiele et al. [4], where calculations for finite temperature conditions at moderate degeneracy are given. We refer for details to that paper and take the traditional Born-Mermin results as a reference point for the inclusion of local field effects. Using the extended Born-Mermin approach together with a static local field correction shows a drastic change in the dispersion relation for larger values of k. This is expected from Fig. 2, where $G_{ee}(k)$ shows considerable deviations from the RPA limit, i.e. $G_{ee}(k) = 0$. Also, the larger local field factor for increasing r_s leads to a more pronounced change in the dispersion relation, as can be seen by comparing the three values of r_s. However, once we refine the approximation by allowing for dynamic local field corrections, these drastic changes disappear again and a dispersion close to the original Born-Mermin curve is found, at least for $r_s = 1$ and $r_s = 2$. In the case of $r_s = 5$, noticeable differences from both, BM and BM+sLFC remain. This behavior can be understood by inspection of the frequency dependence of $\mathrm{Re}\, G(k, \omega)$. While $\mathrm{Re}\, G(k, 0)$ increases with k, $\mathrm{Im}\, G(k, \infty)$ is considerably smaller or even negative for large k, see e.g. [30]. As a consequence, values at intermediate frequencies are considerable smaller than the static value $\mathrm{Re}\, G(k, 0)$. For larger values of k, a zero is even found corresponding to a RPA-like behavior at this frequency. We illustrate this fact in Fig. 10, showing the real and the imaginary part of the dynamic local field correction as a function of the frequency ω for $k = k_F$ and $r_s = 2$. Note however, that the dispersion relation is somewhat misleading. A frequency scan of the dynamic structure factor reveals a rich structure, which can not adequately represented by a shift and a width only.

Finally, we investigate the plasmon width at $r_s = 5$ for the three different approximations. Again, at $k = 0$, the broadening is only due to the collision frequency. For $k > k_0$, the rapid increase of the broadening with k is due to the RPA contribution. At finite k, local field effects also contribute. In particular, the imaginary part of the dynamic local field correction adds to the total width of the plasmon, if one compares the BM + dLFC result to the BM curve. However, the net effect is not simply the sum of both contributions due to the involved arithmetics of the Mermin expression. This also is revealed by the BM + sLFC result, which deviates noticeably from the BM although no additional imaginary part for $G(k)$ is taken into account.

V. CONCLUSIONS

We devise an interpolation scheme which incorporates electron-ion collisions as well as electron-electron correlations by an extended Mermin approach. We apply this to an interacting electron gas at $T = 0$ interacting with an inert ion background. As inputs act a dynamical collision frequency in Born approximation and different models for dynamic

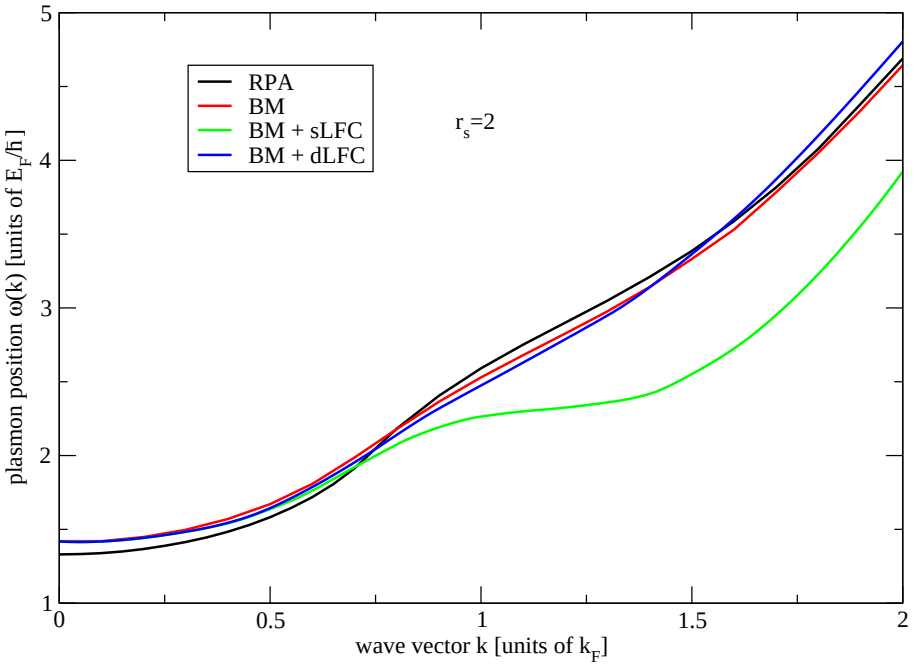

FIG. 8: Plasmon shift $\omega(k)$ as a function of the wave vector k. $r_s = 2$ is studied. BM: traditional Born-Mermin approximation. BM + sLFC: Born-Mermin including static local field corrections. BM + dLFC: Born-Mermin including dynamic local field corrections.

local field corrections of the interacting OCP electron gas. Plasmon properties serve as a probe for the relevance of collisions and correlations, respectively.

At small wave vectors, we observe a dominance of collisions. The importance of local field corrections increase with increasing Brueckner parameter r_s. For $r_s = 5$ it is indispensable to account for local field correlations. Drastic changes in the plasmon properties which occur by taking account of static local field corrections disappear to some extent when using models for dynamic local field corrections. The plasmon broadening shows in general a very involved behavior, collisions and corrections to do not simply add up.

To apply our model to a realistic situation of Thomson scattering in cold matter, we have to refine the input quantities such as the collision frequency and the model for the OCP local field corrections. At this point, there is certainly some improvement to be done.

Our approach can also serve as an approach to study the interplay of impurity scattering and electron-electron correlation in a jellium model description of metals. Here, connection can be made to experimental results for the dynamic structure factor measured by inelastic x-ray scattering [36].

Acknowledgments

This work was supported by the Deutsche Forschungsgemeinschaft (DFG) within the Sonderforschungsbereich SFB 652.

[1] S. H. Glenzer, G. Gregori, R. W. Lee, F. Rogers, S. W. Pollaine, and O. L. Landen, Phys. Rev. Lett. **90**, 175002 (2003).
[2] A. Höll, R. Redmer, G. Röpke, and H. Reinholz, Eur. Phys. J. D 29, 159 (2004).
[3] S. H. Glenzer, O. L. Landen, P. Neumayer, R. W. Lee, K. Widmann, S. W. Pollaine, R. J. Wallace, G. Gregori, A. Höll, T. Bornath, R. Thiele, V. Schwarz, W.-D. Kraeft, and R. Redmer, Phys. Rev. Lett. 98, 065002 (2007).
[4] R. Thiele, T. Bornath, C. Fortmann, A. Höll, R. Redmer, H. Reinholz, G. Röpke, A. Wierling, S.H. Glenzer, and G. Gregori, Phys. Rev. E **78**, 026411 (2008).
[5] J. Chihara, J. Phys. F: Met. Phys. 17, 295 (1987).
[6] S. Ichimaru, Rev. Mod. Phys. **54**, 1017 (1982).
[7] N.D. Mermin, Phys. Rev. B **1**, 2362 (1973).

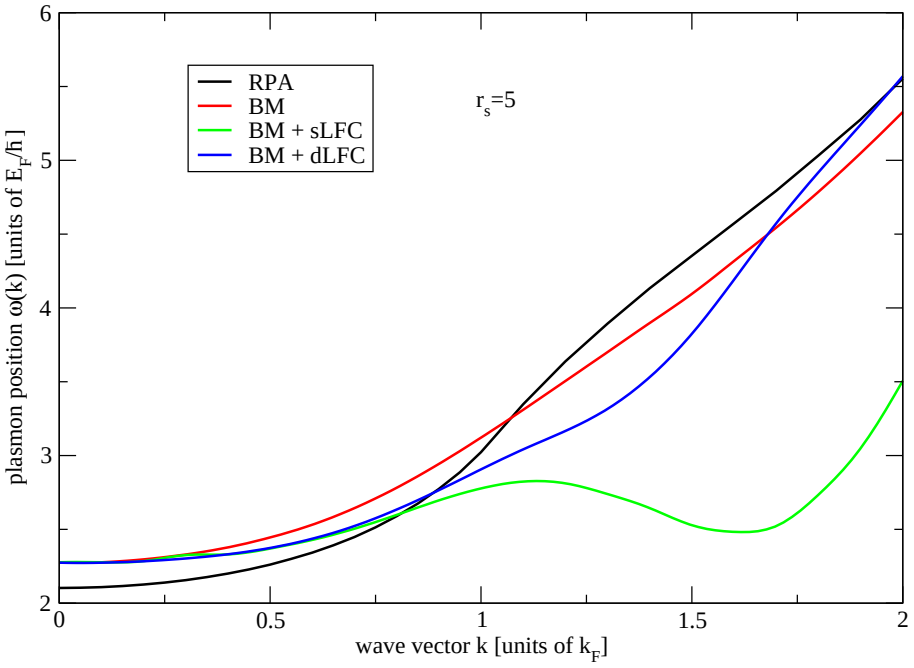

FIG. 9: Plasmon shift $\omega(k)$ as a function of the wave vector k. $r_s = 5$ is studied. BM: traditional Born-Mermin approximation. BM + sLFC: Born-Mermin including static local field corrections. BM + dLFC: Born-Mermin including dynamic local field corrections.

[8] A. Wierling, arXiv:0812.3835 (2008); J. Phys. A: Math. Theor. **42**, 214051 (2009).
[9] D. Zubarev, V. Morozov, and G. Röpke, *Statistical Mechanics of Nonequilibrium Processes*, Vol. 2 (Akademie-Verlag, Berlin, 1997).
[10] G. Röpke, A. Selchow, A. Wierling, and H. Reinholz, Phys. Lett. A **260**, 365 (1999).
[11] S. Ichimaru, S. Mitake, S. Tanaka, and X.-Z. Yan, Phys. Rev. A **32** 1768 (1985)
[12] J. Daligault and M.S. Murillo, Phys. Rev. E **68**, 015401 (2003).
[13] S.V. Adamyan, I.M. Tkachenko, J.L. Munoz-Cobo Gonzalez, and G. Verdu-Martin, Phys. Rev. E **48**, 2067 (1993);
[14] G. Röpke, R. Redmer, A. Wierling, and H. Reinholz, Phys. Rev. E **60**, R2484 (1999).
[15] H. Reinholz, R. Redmer, G. Röpke, and A. Wierling, Phys. Rev. E **62**, 5648 (2000).
[16] N.R. Arista and W. Brandt, Phys. Rev. A **29**, 1471 (1984).
[17] M.D. Barriga-Carrasco, Phys. Rev. E **79**, 027401 (2009).
[18] J. Hubbard, Proc. R. Soc. London Ser. A **243**, 336 (1957).
[19] K. Utsumi and S. Ichimaru, Phys. Rev. B **22**, 5203 (1980).
[20] B. Farid, V. Heine, G.E. Engel, and I.J. Robertson, Phys. Rev. B **48**, 11602 (1993).
[21] S. Ichimaru, *Statistical Plasma Physics*, Vol. II (Addison-Wesley, Reading, 1994).
[22] E. Engel and S.H. Vosko, Phys. Rev. B **42**, 4940 (1990).
[23] K. Singwi, M.P. Tosi, R.H. Land, and A. Sjölander, Phys. Rev. **176**, 589 (1968);
[24] S. Moroni, D.M. Ceperley, and G. Senatore, Phys. Rev. Lett. **75**, 689 (1995).
[25] A. Holas, in *Strongly Coupled Plasma Physics*, ed. by F.J. Rogers and H.E. DeWitt (Plenum, New York, 1987).
[26] B. Dabrowski, Phys. Rev. B **34**, 4989 (1986).
[27] J. Hong and M.H. Lee, Phys. Rev. Lett. **55**, 2375 (1985).
[28] C.F. Richardson and N.W. Ashcroft, Phys. Rev. B **50**, 7284 (1994).
[29] M.H. Lee and J. Hong, J. Phys.: Condens. Matter **1**, 3867 (1989).
[30] N. Iwamoto, E. Krotscheck, and D. Pines, Phys. Rev. B **29**, 3936 (1984).
[31] A.J. Glick and W.F. Long, Phys. Rev. B **4**, 3455 (1971).
[32] E.K.U. Gross and W. Kohn, Phys. Rev. Lett. **55**, 2850 (1985).
[33] In difference to [27], a factor of z has been included into the definition of c_2^0. Furthermore, $-iz$ is used instead of z.
[34] P. Gori-Giorgi, F. Sacchetti, and G.B. Bachelet, Phys. Rev. B **61**, 7353 (2000).
[35] A. Wierling, to be published.
[36] Early works are e.g. P.M. Platzman and P. Eisenberger, Phys. Rev. Lett. **33**, 152 (1974); P.E. Batson and J. Silcox, Phys. Rev. B **27**, 5224 (1983). For a recent review, see W. Schülke, J. Phys.: Condens. Matter **13**, 7557 (2001).

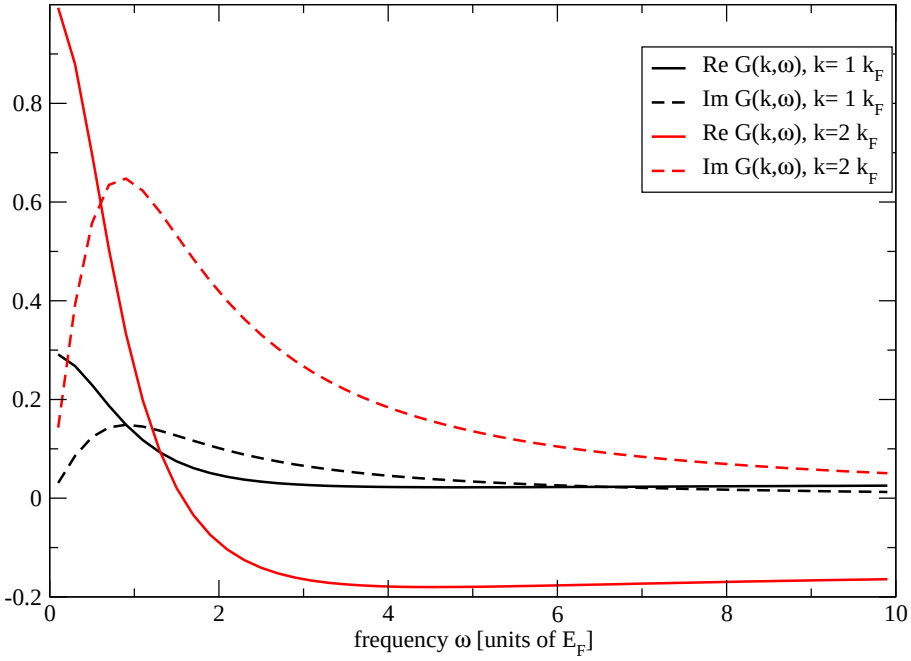

FIG. 10: Real and imaginary part for dynamic local field correction at r_s=2 for two different wave vectors as a function of the frequency.

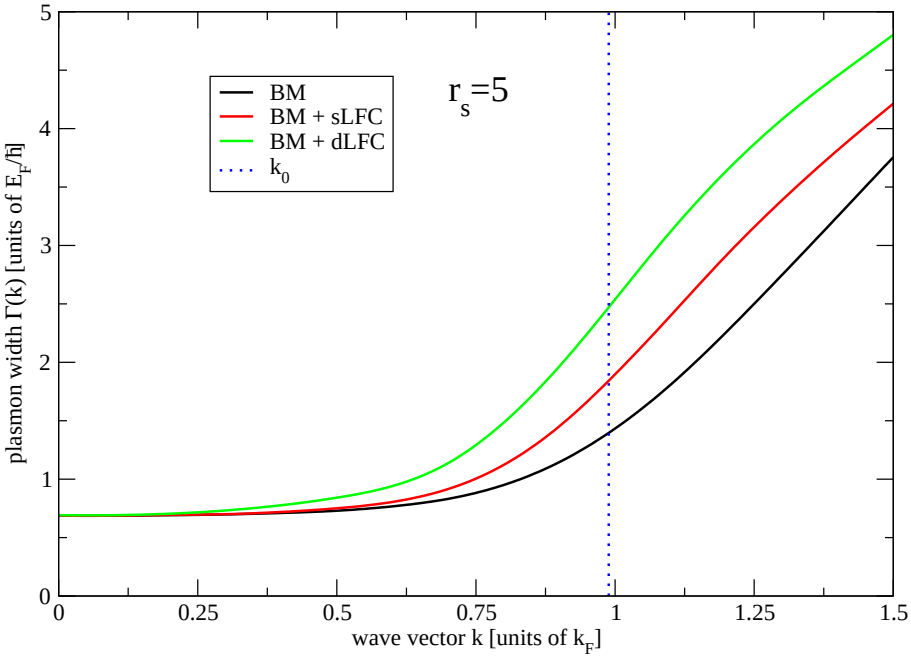

FIG. 11: Plasmon width $\omega(k)$ as a function of the wave vector k. $r_s = 5$ is studied. The traditional Born-Mermin without local field corrections is compared to the extended approach with static (BM + sLFC) and dynamic local field corrections (BM + dLFC). The onset k_0 of the single-particle excitations in RPA is also shown.